IEEE Access
Multidisciplinary : Rapid Review : Open Access Journal

Received January 23, 2019, accepted February 5, 2019, date of publication February 18, 2019, date of current version March 18, 2019.

Digital Object Identifier 10.1109/ACCESS.2019.2899900

Multidimensional Joint Domain Localized Matrix Constant False Alarm Rate Detector Based on Information Geometry Method With Applications to High Frequency Surface Wave Radar

LEI YE[1], QIANG YANG[1,2], QIUSHI CHEN[1], AND WEIBO DENG[1,2]
[1]Department of Electronic and Information Engineering, Harbin Institute of Technology, Harbin 150001, China
[2]Key Laboratory of Marine Environmental Monitoring and Information Processing, Ministry of Industry and Information Technology, Harbin 150001, China

Corresponding author: Qiang Yang (yq@hit.edu.cn)

This work was supported in part by the National Natural Science Foundation of China under Grant 61171182 and Grant 61032011, and in part by the Fundamental Research Funds for the Central Universities under Grant HIT.MKSTISP.2016 13 and Grant HIT.MKSTISP.2016 26.

ABSTRACT This paper proposes a joint domain localized matrix constant false alarm rate detector based on the space-time adaptive processing and information geometry method to improve the detection performance for high-frequency surface wave radar. Unlike traditional target detectors that use one-dimensional or two-dimensional amplitude information, the proposed detector considers multidimensional information of the signal to easily distinguish the target from the noise or clutter. The multidimensional information is obtained by joint domain localized processing, a reduced dimension space-time adaptive algorithm. Then using the information geometry method, we map the detection problem to the geometric manifold and detect the targets by geometric measures. This paper proposes different detectors based on different geometric measures. The experiments and results show that the proposed detectors can enhance the detection performance compared with classical cell average constant false alarm rate detector.

INDEX TERMS Radar applications, radar detection, information entropy, detectors, multidimensional signal processing, radar signal processing, adaptive signal processing, information geometry.

I. INTRODUCTION

High frequency surface wave radar (HFSWR) utilizes high-frequency band (3-30MHz) electromagnetic waves which propagate along the ocean surface to monitor the surface or detect low altitude targets. This radar has the advantages of being all-weather, over-the-horizon and has a large detection range [1], [2]. However, the increase in target distance and the influence of clutter degrades the signal-to-clutter ratio (SCR), thus reducing target detection performance. Therefore, the improvement of the detection performance for a low SCR has practical significance. Many studies have been conducted to solve this problem. In [3], an ensemble constant false alarm rate (CFAR) detector was proposed by Srinivasan. Turley [4] presented a CFAR detector based on hybrid techniques. Further, in [5]–[7], a CFAR detector with matrix-valued observations was proposed. However, most of these detectors are based on one-dimensional or two-dimensional amplitude information from the radar signal. This paper presents a detector based on the multidimensional signal information that can effectively improve the detection performance.

To obtain the velocity and azimuth dimension information from the signal, joint domain localized (JDL) processing, a space time processing algorithm, is applied. References [8] and [9] first applied JDL processing algorithm to airborne surveillance radars, and [10] presented a JDL generalized likelihood ratio (JDL-GLR) detector for airborne radars. In this study, we used JDL processing to obtain covariance matrices that contain the information on velocity and azimuth of the target and clutter. Then we constructed a detector structure in the range dimension. Therefore, after the

The associate editor coordinating the review of this manuscript and approving it for publication was Gerard-Andre Capolino.

targets are detected, the range, velocity, and azimuth information of the targets can be obtained. Instead of using amplitude information from the received signal, we used the covariance matrix of the data, including multidimensional information on target and clutter. Because more information is utilized, the target can be detected from the clutter or noise more easily. Moreover, we used the geometric distance to distinguish the target from clutter, which can give the detector a geometric meaning and interpretation.

To construct the detector in the range dimension, covariance matrices with multidimensional information can be retrieved by using the Hermitian positive-definite (HPD) matrices [16], which can be mapped to a manifold by the information geometry method. The concept of information geometry, based on information theory, geometry, and statistics, was proposed by Rao in 1945 [11]. Many scholars have researched the theory and applied it to statistical inference, neural network, pattern analysis, signal processing, etc. [12]–[15]. Based on the information geometry method, five different geometric measures were used to realize the JDL matrix constant false alarm rate (JDL-MCFAR) detector. The detector constructed by the information geometry method, based on the multidimensional information of the signal, can improve detection performance.

The remainder of this paper is organized as follows. In Section 2, HPD matrices are constructed using the JDL processing algorithm. Section 3 proposes the matrix CFAR detector and presents five different detectors based on different geometric measures. The simulations and results are presented in Section 4. The study is concluded in Section 5.

A. NOTATION

The notations adopted in this paper are as follows. Math italic is used to represent scalars (x), uppercase boldface denotes matrices ($\boldsymbol{X}$), lowercase boldface denotes vectors ($\boldsymbol{x}$), and blackboard bold indicates a set of matrices $\mathbb{R}$. $(\cdot)^T$, $(\cdot)^*$, $(\cdot)^H$,$\otimes$, $E[\cdot]$, $tr(\cdot)$, and $\det(\cdot)$, denote the transpose operator, conjugate operator, conjugate transpose operator, the Kronecker product operator, expectation operator, trace, and determinant of the matrix, respectively. $\boldsymbol{I}$ represents the identity matrix.

II. CONSTRUCTION OF HPD MATRICES BY JDL ALGORITHM

Consider a receiving antenna array of a HFSWR with N channels, as shown in Figure 1. Each channel receives M sample data corresponding to a train of M pulses per coherent processing interval (CPI) for a certain range cell. The sample data vector of each channel is given as $\boldsymbol{x}_{tn} = [x_{tn1}, x_{tn2}, \cdots, x_{tnM}]^T$ and $\boldsymbol{x}_{sm} = [x_{sm1}, x_{sm2}, \cdots, x_{smN}]^T$ is the channel data vector of each pulse. Therefore, the data matrix $\mathbf{X}$ with N*M dimension can be defined as:

$$\boldsymbol{X} = [\boldsymbol{x}_{t_1}, \boldsymbol{x}_{t_2}, \cdots, \boldsymbol{x}_{t_N}] = \begin{bmatrix} \boldsymbol{x}_{s_1}^T \\ \boldsymbol{x}_{s_2}^T \\ \vdots \\ \boldsymbol{x}_{s_M}^T \end{bmatrix} \quad (1)$$

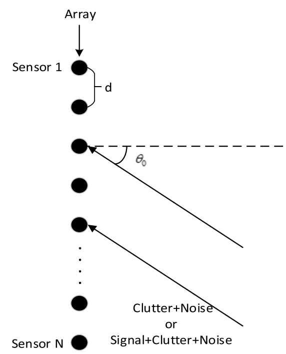

FIGURE 1. Receiving array of a HFSWR.

The row vector $[\boldsymbol{x}_{t_1}, \boldsymbol{x}_{t_2}, \cdots, \boldsymbol{x}_{t_N}]$ is the sample data vector of N channels, and the column vector $[\boldsymbol{x}_{s_1}, \boldsymbol{x}_{s_2}, \cdots, \boldsymbol{x}_{s_M}]^T$ is the channel data vector of M pulses.

Under hypothesis H_0, without the signal, the data matrix $\boldsymbol{X}$ contains only clutter and noise:

$$\boldsymbol{X} = \boldsymbol{C} + \boldsymbol{N}, \quad (2)$$

where $\boldsymbol{C}$ denotes clutter and $\boldsymbol{N}$ represents noise. They are both assumed to be independent, and their models are Gaussian models. Under the signal-presence hypothesis H_1, the data matrix $\boldsymbol{X}$ is consisted of signal, clutter, and noise:

$$\boldsymbol{X} = \alpha\boldsymbol{S} + \boldsymbol{C} + \boldsymbol{N}, \quad (3)$$

where $\boldsymbol{S}$ represents the signal, and α is an unknown constant that denotes the amplitude of the signal. The data matrix $\boldsymbol{X}$ is the primary data set from the range cell. For the JDL processing, the data matrix $\boldsymbol{X}$ is processed to obtain the information in the azimuth-Doppler domain, and then, to detect the target in the same domain.

For simplicity, it is assumed that the array elements are identical, collinear, and equidistant. Thus, the transformed data at Doppler frequency f_{d0} and azimuth θ_0 can be obtained by:

$$y_0(\theta_0, f_{d0}) = \boldsymbol{w}^H\boldsymbol{x} \quad (4)$$

$$\boldsymbol{w} = w_s(\theta_0) \otimes w_t(f_{d0}) \quad (5)$$

$$w_s(\theta_0) = e^{j2\pi(d/\lambda)sin(\theta_0)[0,1,\cdots,N-1]^T} \quad (6)$$

$$w_t(f_{d0}) = e^{j2\pi f_{d0}T_p[0,1,\cdots,M-1]^T} \quad (7)$$

where $\boldsymbol{x}$ is a vectorization of $\boldsymbol{X}$ with the dimension N*$M \times 1$, $w_s(\theta_0)$ is the steering vector with azimuth θ_0 in the space domain, and $w_t(f_{d0})$ is the steering vector with the Doppler frequency f_{d0} in the time domain. λ is the wavelength of the electromagnetic wave, T_p is the pulse repetition period, and $y_0(\theta_0, f_{d0})$ is the output data at the azimuth θ_0 and frequency f_{d0}.

The output data of the transformation is presented in Figure 2 (a). Each point in the azimuth-Doppler domain is transformed from the primary data vector. A localized processing region (LPR) consists of $n_a * n_d$ points. Figure 2 (b) depicts the clutter reference cells for a certain LPR. Utilizing the JDL processing, we can calculate the covariance matrix of the LPR for the matrix detector.

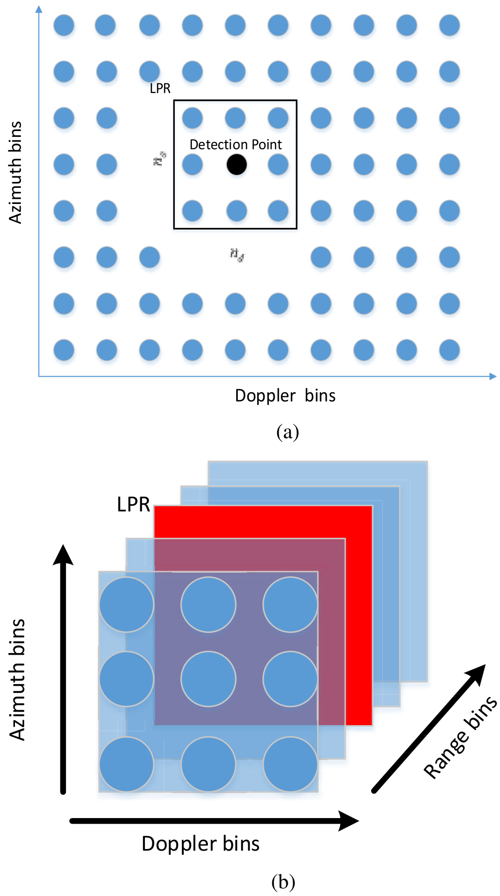

FIGURE 2. **Localized processing region. (a) A LPR in the azimuth-Doppler dimension. (b) A LPR and its clutter reference cells in range dimension.**

The LPR with n_a azimuth bins and n_d Doppler bins can constitute the vector data $\boldsymbol{Y}_n$ with the dimension $n_a * n_d \times 1$. The number of cells used in the local region is 3*3 ($n_a = 3$, $n_d = 3$). This implies that three beams and three Doppler shifts are chosen in one range cell, and the data constitute the vector data with the dimension of $9 \times 1(n_a{*}n_d \times 1)$. Therefore, we can estimate the covariance matrix of the LPR with the dimension of 9×9. In [34], it was verified that the dimension 3*3 in the local region is suitable for HFSWR data. The covariance matrix of the LPR is $\boldsymbol{R}_n = E[\boldsymbol{Y}_n \boldsymbol{Y}_n^H]$, which can be obtained by using a structured HPD matrix completion model [16]–[18], [35]. It can be calculated by

$$\boldsymbol{R}_n = \begin{bmatrix} c_0 & c_1^* & \cdots & c_{n-1}^* \\ c_1 & c_0 & \ddots & \vdots \\ \vdots & \vdots & \ddots & c_1^* \\ c_{n-1} & \cdots & c_1 & c_0 \end{bmatrix} \textit{with } c_k = E[y_n y_{n+k}^*] \tag{8}$$

where y_n denotes the element of LPR, y_{n+k}^* represents the conjugate of y_{n+k} and c_k is the correlation coefficient. The coefficient can be calculated by averaging in the time domain, instead of statistical expectation as

$$c_k = \frac{1}{n} \sum_{n=0}^{n-1-k} y(n) y^*(n+k), \; k \le n-1 \tag{9}$$

Similarly, the HPD covariance matrices of the reference units can be obtained.

Let $\mathbb{P}(n)$ denote the set of the all $n \times n$ HPD matrices, and it can be described by

$$\mathbb{P}(n) = \{\boldsymbol{R} \in \mathbb{H}(n), \boldsymbol{R} > 0\}, \tag{10}$$

where $\mathbb{H}(n)$ denotes the space of all $n \times n$ Hermitian matrices, and $\mathbb{P}(n)$ can form a differentiable Riemannian manifold [19], [20], which is a symmetric space with a non-positive curvature [21]. Thus, the covariance matrices of the detection unit and reference units can be projected onto the geometric manifold through the information geometry theory. Whether the target is in the detection unit can be predicted by their distance.

III. MATRIX CFAR DETECTOR

In this section, the structure of JDL-MCFAR detector is described, and then, some distance measures and the mean matrix are presented.

As the HPD matrices obtained by the JDL processing can construct a differentiable Riemannian manifold, the detector can be built based on the manifold. We can obtain the mean matrix $\bar{\boldsymbol{R}}$ of the reference units, and then, calculate the geometric distance between the covariance matrix of the detection unit $\boldsymbol{R}_0$ and the mean matrix $\bar{\boldsymbol{R}}$. By Comparison with a threshold, the target's existence can be judged:

$$\begin{cases} H_1 \; : \; d(\boldsymbol{R}_D, \bar{\boldsymbol{R}}) > T \\ H_0 \; : \; d(\boldsymbol{R}_D, \bar{\boldsymbol{R}}) < T \end{cases} \tag{11}$$

where $d(\boldsymbol{R}_D, \bar{\boldsymbol{R}})$ is the geometric distance between the detection matrix and the mean matrix, T is the detection threshold, H_1 denotes the presence of the target, and H_0 denotes the absence.

The structure of the JDL-MCFAR detector is represented in Figure 3. Compared with the classical CFAR detector, the JDL-MCFAR detector can obtain multidimensional information of the target and clutter by JDL processing. Thus, the detector can discriminate the target from the clutter more easily. The geometric illustration is shown in Figure 4, where $\boldsymbol{R}_{D0}$ is the detection matrix without target, $\boldsymbol{R}_{D1}$ is the detection matrix with the target, $\boldsymbol{R}_1, \boldsymbol{R}_2, \cdots, \boldsymbol{R}_N$ are the covariance matrices of the reference units, and $\bar{\boldsymbol{R}}$ is the mean matrix of $\boldsymbol{R}_1, \boldsymbol{R}_2, \cdots, \boldsymbol{R}_N$. We can observe that the distance between the detection matrix and the mean matrix of the reference units will be longer if there exists target. Consequently, whether there is target in the detection unit or not can be verified by comparing the distance with a certain threshold.

Two important concepts should be considered: the distance between two matrices, and the mean matrix. In this study, five different distance measures, Riemannian distance, Kullback Leibler divergence [22], log determinant divergence [23],

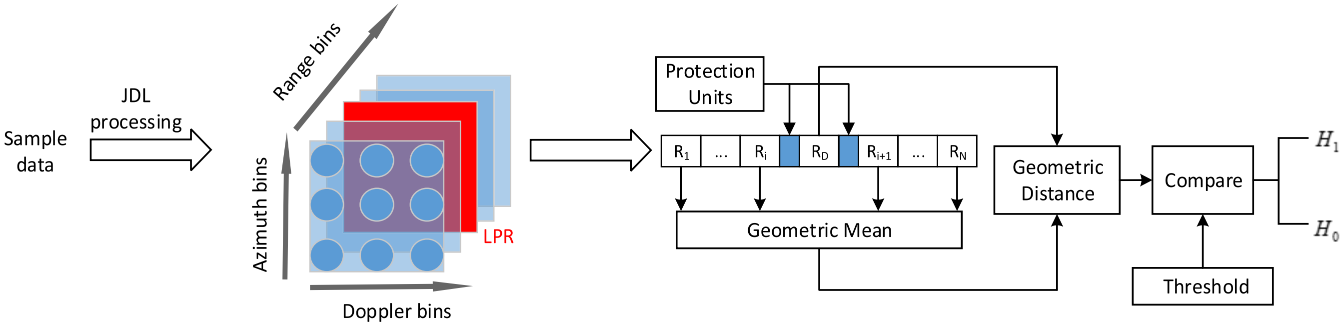

FIGURE 3. **The structure of the JDL-MCFAR detector.**

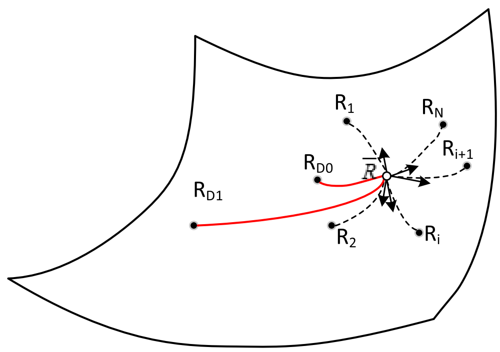

FIGURE 4. **Geometric illustration of JDL-MCFAR detector on a manifold.**

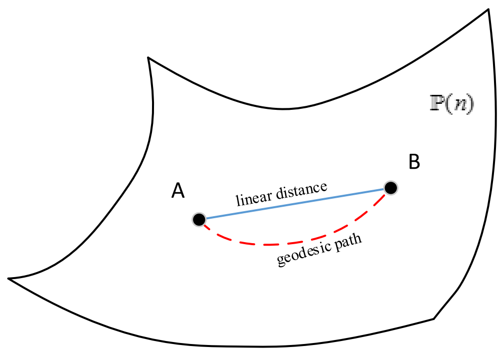

FIGURE 5. **Geodesic distance and linear distance on a manifold.**

Bhattacharyya distance [24], and Hellinger distance [25] are used, and corresponding mean matrices based on these distance measures are deduced.

A. DISTANCE BETWEEN MATRICES

The method used to measure the distance between two matrices is an important criterion for the JDL-MCFAR detector. As shown in Figure 5, A and B denote two points on the manifold $\mathbb{P}(n)$ constructed using the HPD matrix, and the distance between them needs to be measured. In the Euclidean space, the shortest distance between two points is the linear distance between the points. Similarly, the shortest distance between two points in the geometric manifold space is the geodesic distance.

1) RIEMANNIAN DISTANCE (RD)

The geodesic distance is a basic distance metric with respect to the geometric construction of a manifold. As the geodesic distance can be calculated by the Riemannian metric, it is also called as Riemannian distance (RD). As $\mathbb{P}(n)$ is a differential manifold with tangent space $\mathbb{T}_A$ at point A, the differential arclength at point $\boldsymbol{A}$ is given as

$$ds := \left(tr(\boldsymbol{A}^{-1}d\boldsymbol{A})^2\right)^{1/2} = \left\|\boldsymbol{A}^{-1/2}d\boldsymbol{A}\boldsymbol{A}^{-1/2}\right\|_F \tag{12}$$

Here, the prefix d denotes the differential operator. Equation (12) defines a metric on the differential manifold $\mathbb{P}(n)$, and the inner product of the tangent space $\mathbb{T}_A$ can be defined as follows [26]–[28]:

$$\langle \boldsymbol{R}_1, \boldsymbol{R}_2 \rangle_A = tr(\boldsymbol{A}^{-1}\boldsymbol{R}_1\boldsymbol{A}^{-1}\boldsymbol{R}_2) \tag{13}$$

To measure the Riemannian distance between $\boldsymbol{R}_1$ and $\boldsymbol{R}_2$ on the manifold, an effective method is given by [29] and can be written as:

$$\begin{aligned} D_R{}^2(\boldsymbol{R}_1, \boldsymbol{R}_2) &= \| \log(\boldsymbol{R}_1{}^{-1}\boldsymbol{R}_2) \|_F^2 \\ &= \| \log(\boldsymbol{R}_1{}^{-1/2}\boldsymbol{R}_2\boldsymbol{R}_1{}^{-1/2}) \|_F^2 \\ &= tr[\log^2(\boldsymbol{R}_1{}^{-1/2}\boldsymbol{R}_2\boldsymbol{R}_1{}^{-1/2})] \\ &= \sum_{k=1}^{n} \log^2(\lambda_k) \end{aligned} \tag{14}$$

where λ_k is the eigenvalue of the matrix $\boldsymbol{R}_1{}^{-1/2}\boldsymbol{R}_2\boldsymbol{R}_1{}^{-1/2}$, and $\| \boldsymbol{R} \|_F^2 = \langle \boldsymbol{R}, \boldsymbol{R} \rangle = tr(\boldsymbol{R}\boldsymbol{R}^T)$.

In addition to the Riemannian metric, many other distance or divergence measures can be used on the manifold $\mathbb{P}(n)$. Here, four other measures are utilized for distance calculation.

2) KULLBACK-LEIBLER DIVERGENCE (KLD)

In information geometry theory, the KLD is typically used to measure the difference between two probability distributions. The divergence can act as a measure of the distance between two points. The effective method to calculate the KLD between two matrices is given as

$$\begin{aligned} D_{KL}(\boldsymbol{R}_1, \boldsymbol{R}_2) &= tr(\boldsymbol{R}_2^{-1}\boldsymbol{R}_1 - I) - \log\det(\boldsymbol{R}_2^{-1}\boldsymbol{R}_1) \\ &= \sum_{i=1}^{n} (\lambda_i - \log\lambda_i - 1) \end{aligned} \tag{15}$$

Here, λ_i is the eigenvalue of the matrix $\boldsymbol{R}_2^{-1}\boldsymbol{R}_1$.

3) LOG DETERMINANT DIVERGENCE (LDD)

The Log determinant divergence is also known as Stein's loss [30], which is widely used in machine learning and information theory. The LDD of two matrices on a manifold is defined as follows:

$$D_{LD}(\boldsymbol{R}_1, \boldsymbol{R}_2) = tr(\boldsymbol{R}_2^{-1}(\boldsymbol{R}_1 - \boldsymbol{R}_2)) - \log\det(\boldsymbol{R}_2^{-1}\boldsymbol{R}_1) \quad (16)$$

It is should be noted here that the KLD and LDD are not strictly definitions of distance, as they neither satisfy the symmetry property nor the triangle inequality. Nevertheless, they can be used in our detector to compare the divergence between two matrices on the manifold.

4) BHATTACHARYYA DISTANCE (BD)

The Bhattacharyya distance was originally defined by Bhattacharyya [24] and can be used in statistics to measure the similarity between two probability distributions. The BD of two covariance matrices can be written as

$$D_B(\boldsymbol{R}_1, \boldsymbol{R}_2) = 2\sqrt{\log \frac{\det((\boldsymbol{R}_1 + \boldsymbol{R}_2)/2)}{\sqrt{\det(\boldsymbol{R}_1)\det(\boldsymbol{R}_2)}}} \quad (17)$$

5) HELLINGER DISTANCE (HD)

The Hellinger distance is another effective measure to obtain the distance between two points on a differential manifold, and it is defined as [25]

$$D_H(\boldsymbol{R}_1, \boldsymbol{R}_2) = \sqrt{2 - 2\frac{\det(\boldsymbol{R}_1)^{1/4}\det(\boldsymbol{R}_2)^{1/4}}{\det((\boldsymbol{R}_1 + \boldsymbol{R}_2)/2)^{1/2}}} \quad (18)$$

B. MEAN MATRIX

The mean matrix is the average of the covariance matrices of the reference units. It reflects the mean information of the reference units compared to the detection unit. The geometric mean of the covariance matrices was originally defined by Pennec, and Karcher subsequently proved that the geometric mean exist and is unique for a manifold with non-positive curvature [31]. The geometric mean is an average method to obtain the local minimum value of the objective function represented by empirical variance, and can be defined as

$$\begin{aligned} \bar{R} &= \arg\min_{\boldsymbol{R}\in\mathbb{P}(n)} F(\boldsymbol{R}_1, \boldsymbol{R}_2, \cdots, \boldsymbol{R}_N) \\ &= \arg\min_{\boldsymbol{R}\in\mathbb{P}(n)} \frac{1}{N}\sum_{k=1}^{N} d^2(\boldsymbol{R}_k, \boldsymbol{R}) \end{aligned} \quad (19)$$

where $F(\boldsymbol{R}_1, \boldsymbol{R}_2, \cdots, \boldsymbol{R}_N)$ denotes the objective function represented by empirical variance, and $d(\boldsymbol{R}_k, \boldsymbol{R})$ indicates the distance between two matrices $\boldsymbol{R}_k$ and $\boldsymbol{R}$. For the different distance measures presented in Section 3.1, the corresponding geometric means are obtained as follows:

1) RIEMANNIAN MEAN

Based on the Jacobi field, [32] provides an iterative gradient descent algorithm that can be used to calculate the Riemannian mean effectively as follows:

$$\begin{aligned} \bar{\boldsymbol{R}}_{t+1} &= \bar{\boldsymbol{R}}_t^{\frac{1}{2}} \exp[-ds\bar{\boldsymbol{R}}_t^{-\frac{1}{2}} \nabla F(\boldsymbol{R}_1, \boldsymbol{R}_2, \cdots, \boldsymbol{R}_N)\bar{\boldsymbol{R}}_t^{-\frac{1}{2}}]\bar{\boldsymbol{R}}_t^{\frac{1}{2}} \\ &= \bar{\boldsymbol{R}}_t^{\frac{1}{2}} \exp[-ds\frac{\bar{\boldsymbol{R}}_t^{\frac{1}{2}}}{N}\sum_{k=1}^{N} \log(\boldsymbol{R}_k^{-1}\bar{\boldsymbol{R}}_t)\bar{\boldsymbol{R}}_t^{-\frac{1}{2}}]\bar{\boldsymbol{R}}_t^{\frac{1}{2}} \\ &= \bar{\boldsymbol{R}}_t^{\frac{1}{2}} \exp[ds\frac{1}{N}\sum_{k=1}^{N} \log(\bar{\boldsymbol{R}}_t^{-\frac{1}{2}}\boldsymbol{R}_k\bar{\boldsymbol{R}}_t^{-\frac{1}{2}})]\bar{\boldsymbol{R}}_t^{\frac{1}{2}} \end{aligned} \quad (20)$$

where N is the dimension of each covariance matrix, ds is the step size, $\bar{\boldsymbol{R}}_t$ is the estimation of the mean for iteration t, and $\bar{\boldsymbol{R}}_{t+1}$ is the estimation at iteration $t+1$. Then, the Riemannian mean can be obtained using an appropriate number of iterations.

Similarly, the geometric means of the other measures can be obtained according to the definition [33]. Let the objective function $F(\boldsymbol{R}_1, \boldsymbol{R}_2, \cdots, \boldsymbol{R}_N) = \frac{1}{N}\sum_{i=1}^{N} d^2(\boldsymbol{R}, \boldsymbol{R}_i)$, and let the gradient function $\nabla F(\boldsymbol{R}_1, \boldsymbol{R}_2, \cdots, \boldsymbol{R}_N)$ be set as zero. Then, we separate $\boldsymbol{R}$ to the left of the function; in this manner, the solution of the geometric means can be calculated.

2) KULLBACK-LEIBLER MEAN

According to the KLD, the objective function is

$$\begin{aligned} &F(\boldsymbol{R}_1, \boldsymbol{R}_2, \cdots, \boldsymbol{R}_N) \\ &\quad = 1N\sum_{i=1}^{N}\left(tr(\boldsymbol{R}_i^{-1}\boldsymbol{R} - I) - \log\det(\boldsymbol{R}_i^{-1}\boldsymbol{R})\right) \end{aligned} \quad (21)$$

Thus, the gradient function of KLD $\nabla F(\boldsymbol{R}_1, \boldsymbol{R}_2, \cdots, \boldsymbol{R}_N)$ is given by

$$\begin{aligned} &\nabla F(\boldsymbol{R}_1, \boldsymbol{R}_2, \cdots, \boldsymbol{R}_N) \\ &\quad = \nabla\left(\frac{1}{N}\sum_{i=1}^{N}\left[tr(\boldsymbol{R}_i^{-1}\boldsymbol{R} - I) - \log\det(\boldsymbol{R}_i^{-1}\boldsymbol{R})\right]\right) \\ &\quad = \frac{1}{N}\sum_{i=1}^{N}\left(\boldsymbol{R}_i^{-1} - \boldsymbol{R}^{-1}\right) \end{aligned} \quad (22)$$

Then, we set the gradient function to zero, so we can obtain the mean matrix of KLD:

$$\bar{\boldsymbol{R}} = \left(\frac{1}{N}\sum_{i=1}^{N}\boldsymbol{R}_i^{-1}\right)^{-1} \quad (23)$$

3) LOG DETERMINANT MEAN

Similar to the KLD, the gradient function of the LDD is

$$\begin{aligned} &\nabla F(R_1, \boldsymbol{R}_2, \cdots, \boldsymbol{R}_N) \\ &\quad = \nabla\left(\frac{1}{N}\sum_{i=1}^{N}\left[tr(\boldsymbol{R}_i^{-1}(\boldsymbol{R} - \boldsymbol{R}_i)) - \log\det(\boldsymbol{R}_i^{-1}\boldsymbol{R})\right]\right) \\ &\quad = \frac{1}{N}\sum_{i=1}^{N}\left(\boldsymbol{R}_i^{-1} - \boldsymbol{R}^{-1}\right) \end{aligned} \quad (24)$$

TABLE 1. Geometric distance or divergence and mean formulation of different measures.

Measure	Distance or divergence	Geometric mean formulation
RD	$D^2_{\boldsymbol{R}}(\boldsymbol{R}_1,\boldsymbol{R}_2) = tr[\log^2(\boldsymbol{R}_1{}^{-1/2}\boldsymbol{R}_2\boldsymbol{R}_1{}^{-1/2})]$	$\bar{\boldsymbol{R}}_{t+1} = \bar{\boldsymbol{R}}_t^{1/2}\exp[-ds\cdot\frac{\bar{\boldsymbol{R}}_t^{1/2}}{N}\sum_{k=1}^{N}\log(\boldsymbol{R}_k^{-1}\bar{\boldsymbol{R}}_t)\bar{\boldsymbol{R}}_t^{-1/2}]\bar{\boldsymbol{R}}_t^{1/2}$
KLD	$D_{KL}(\boldsymbol{R}_1,\boldsymbol{R}_2) = tr(\boldsymbol{R}_2^{-1}\boldsymbol{R}_1 - I) - lndet(\boldsymbol{R}_2^{-1}\boldsymbol{R}_1)$	$\bar{\boldsymbol{R}} = \left(\frac{1}{N}\sum_{i=1}^{N}\boldsymbol{R}_i^{-1}\right)^{-1}$
LDD	$D_{LD}(\boldsymbol{R}_1,\boldsymbol{R}_2) = tr(\boldsymbol{R}_2^{-1}(R\boldsymbol{R}_1 - \boldsymbol{R}_2)) - lndet(\boldsymbol{R}_2^{-1}\boldsymbol{R}_1)$	$\bar{\boldsymbol{R}} = \left(\frac{1}{N}\sum_{i=1}^{N}\boldsymbol{R}_i^{-1}\right)^{-1}$
BD	$D_B(\boldsymbol{R}_1,\boldsymbol{R}_2) = 2\sqrt{\log\frac{\det(\frac{\boldsymbol{R}_1+\boldsymbol{R}_2}{2})}{\sqrt{\det(\boldsymbol{R}_1)det(\boldsymbol{R}_2)}}}$	$\bar{\boldsymbol{R}}_{t+1} = \left(\frac{1}{N}\sum_{i=1}^{N}\left(\frac{\bar{\boldsymbol{R}}_t+\boldsymbol{R}_i}{2}\right)^{-1}\right)^{-1}$
HD	$D_H(\boldsymbol{R}_1,\boldsymbol{R}_2) = \sqrt{2-2\frac{\det(\boldsymbol{R}_1)^{\frac{1}{4}}\det(\boldsymbol{R}_2)^{\frac{1}{4}}}{\det(\frac{\boldsymbol{R}_1+\boldsymbol{R}_2}{2})^{\frac{1}{2}}}}$	$\bar{\boldsymbol{R}}_{t+1} = \left(\frac{\sum_{i=1}^{N}\lvert\bar{\boldsymbol{R}}_t\rvert^{\frac{1}{4}}\lvert\boldsymbol{R}_i\rvert^{\frac{1}{4}}\left\lvert\frac{(\bar{\boldsymbol{R}}_t+\boldsymbol{R}_i)}{2}\right\rvert^{-\frac{1}{2}}\left(\frac{(\bar{\boldsymbol{R}}_t+\boldsymbol{R}_i)}{2}\right)^{-1}}{\sum_{i=1}^{N}\lvert\bar{\boldsymbol{R}}_t\rvert^{\frac{1}{4}}\lvert\boldsymbol{R}_i\rvert^{\frac{1}{4}}\left\lvert\frac{(\bar{\boldsymbol{R}}_t+\boldsymbol{R}_i)}{2}\right\rvert^{-\frac{1}{2}}}\right)^{-1}$

Thus, the mean matrix of the LDD is

$$\bar{\boldsymbol{R}} = \left(\frac{1}{N}\sum_{i=1}^{N}\boldsymbol{R}_i^{-1}\right)^{-1} \tag{25}$$

4) BHATTACHARYYA MEAN

According to the BD, the objective function is

$$F(\boldsymbol{R}_1,\boldsymbol{R}_2,\cdots,\boldsymbol{R}_N) = \frac{1}{N}\sum_{i=1}^{N}4\log\frac{\det((\boldsymbol{R}+\boldsymbol{R}_i)/2)}{\sqrt{\det(\boldsymbol{R})\det(\boldsymbol{R}_i)}} \tag{26}$$

Consequently, the gradient function is given by

$$\begin{aligned}\nabla F(\boldsymbol{R}_1,\boldsymbol{R}_2,\cdots,\boldsymbol{R}_N) &= \nabla\frac{1}{N}\sum_{i=1}^{N}4\left(\log\frac{\det((\boldsymbol{R}+\boldsymbol{R}_i)/2)}{\sqrt{\det(\boldsymbol{R})\det(\boldsymbol{R}_i)}}\right)\\ &= \frac{4}{N}\sum_{i=1}^{N}\left(\left(\frac{\boldsymbol{R}+\boldsymbol{R}_i}{2}\right)^{-1} - \boldsymbol{R}^{-1}\right)\end{aligned} \tag{27}$$

Similar to the KLD, we set the gradient function to zero and separate the matrix $\boldsymbol{R}$. Thus, the mean matrix of BD can be obtained as follows:

$$\bar{\boldsymbol{R}}_{t+1} = \left(\frac{1}{N}\sum_{i=1}^{N}\left(\frac{\bar{\boldsymbol{R}}_t+\boldsymbol{R}_i}{2}\right)^{-1}\right)^{-1} \tag{28}$$

5) HELLINGER MEAN

Similar to the Bhattacharyya mean, we can obtain the Hellinger mean by

$$\bar{\boldsymbol{R}}_{t+1} = \left(\frac{\sum_{i=1}^{N}\lvert\bar{\boldsymbol{R}}_t\rvert^{\frac{1}{4}}\lvert\boldsymbol{R}_i\rvert^{\frac{1}{4}}\left\lvert\frac{(\bar{\boldsymbol{R}}_t+\boldsymbol{R}_i)}{2}\right\rvert^{-\frac{1}{2}}\left(\frac{(\bar{\boldsymbol{R}}_t+\boldsymbol{R}_i)}{2}\right)^{-1}}{\sum_{i=1}^{N}\lvert\bar{\boldsymbol{R}}_t\rvert^{\frac{1}{4}}\lvert\boldsymbol{R}_i\rvert^{\frac{1}{4}}\left\lvert\frac{(\bar{\boldsymbol{R}}_t+\boldsymbol{R}_i)}{2}\right\rvert^{-\frac{1}{2}}}\right)^{-1} \tag{29}$$

Figure 6 shows the changes in the objective functions of the Riemannian, Bhattacharyya and Hellinger means with iteration number, where the identity matrix $\boldsymbol{I}$ is used as the initialization matrix. When the iteration number increases to a certain value, the objective function tends to be stable.

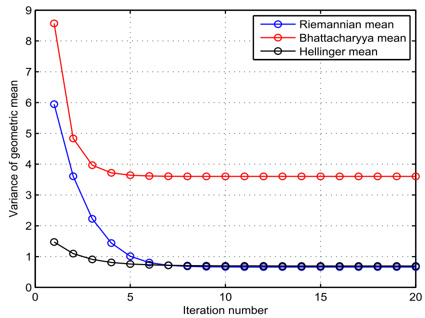

FIGURE 6. The changes in the objective functions of the Riemannian, Bhattacharyya and Hellinger means with iteration number.

The distance and geometric mean matrix formulations of these five measures are summarized in Table 1. Thus, different JDL-MCFAR detectors can be constructed based on the different geometric distances and their mean matrices.

IV. EXPERIMENTS AND RESULTS

In order to evaluate the performance of the detectors introduced in this work, simulations were conducted as follows.

A. COMPUTATIONAL COMPLEXITY OF THE MEASURES

Computational complexity is an important characteristic of signal processing that affects the efficiency of the algorithm and the process itself. Here, we will discuss the complexity of the geometric measures. HFSWR data is of complex-floating-point type, so we evaluate the computational complexity by the number of floating point operations required. Consider HPD matrices $\boldsymbol{R}_1$ and $\boldsymbol{R}_2$ with dimension $n \times n$ each; the computational complexity of these matrices can be calculated as follows.

For instance, $\boldsymbol{R}_1\boldsymbol{R}_2$ is the multiplication of the matrices $\boldsymbol{R}_1$ and $\boldsymbol{R}_2$. For each row of $\boldsymbol{R}_1$, the complex floating point multiplication is performed n^2 times, and complex floating point addition is required $n(n-1)$ times. Four and two floating point multiplication and addition operations are respectively required for each complex floating point multiplication, and a complex floating point addition requires two floating point addition operations. Therefore, the number of floating point operations for a matrix multiplication is $6n^3 + 2n^2(n-1)$, which is equal to $8n^3 - 2n^2$ operations.The number of floating point operations for HPD matrix operations are given in Table 2.

TABLE 2. Number of floating point operations.

Operation	Expression	Number of floating point operations
Matrix multiplication	$\boldsymbol{R}_1\boldsymbol{R}_2$	$8n^3 - 2n^2$
Matrix addition	$\boldsymbol{R}_1 + \boldsymbol{R}_2$	$2n^2$
Matrix trace	$tr(\boldsymbol{R}_1)$	$8n^2 - 6n - 2$
Matrix determinant	$\det(\boldsymbol{R}_1)$	$8n^2 - 2n - 6$
Matrix inverse	$\boldsymbol{R}_1^{-1}$	$8n^3 - 2n^2$
Matrix power	$\boldsymbol{R}_1^{1/2}$	$24n^3 + 2n^2 - 8n$
Matrix exponential	$\exp(\boldsymbol{R}_1)$	$\frac{n^4}{2} + 24n^3 + \frac{3n^2}{2} - n$
Matrix logarithm	$\log(\boldsymbol{R}_1)$	$\frac{n^4}{2} + 25n^3 + n^2 - \frac{3n}{2}$

TABLE 3. Number of floating point operations for measures.

Measure	Number of distance	Number of geometric mean
RD	$\frac{n^4}{2} + 73n^3 + 5n^2 - \frac{31n}{2} - 1$	$\frac{(N+1)n^4}{2} + (41n+88)n^3 - \frac{2N+13}{2} - \frac{3N+18}{2}n$
KLD	$16n^3 + 14n^2 - 8n - 6$	$8(N+1)n^3 - 2n^2$
LDD	$16n^3 + 14n^2 - 8n - 6$	$8(N+1)n^3 - 2n^2$
BD	$28n^2 - 6n^2 - 12$	$8(N+1)n^3 + (4N-2)n^2$
HD	$28n^2 - 6n^2 - 10$	$8(N+1)n^3 + (22N+6)n^2 - 4(N-2)n - 9N - 6$

Based on the HPD matrix operations, the number of floating point operations required for different geometric measures can be obtained. These calculations are shown in Table 3. Here, N is the number of matrices that are used to compute the geometric mean. From the table, we see that the RD measure requires the maximum amount of computation. Therefore, the RD measure has the highest computational complexity. For the computation of the geometric distance, the BD has the lowest computational complexity. The KLD and LDD have the lowest complexities for computation of geometric mean.

B. DETECTION PERFORMANCE

A target is added in the received data of the HFSWR to verify the performance of the detectors for different measures. The parameters of this experiment are as follows. The distance between two sensors (d_A) is 14.5 m, the number of the sensors (N) is 8, the number of coherent pulses (M) is 512, and the frequency is 5.6 MHz. The target is added in the 30^{th} range cell with a Doppler velocity of -4.81m/s and azimuth of 0^o. Figure 7 shows the normalized statistics of different measures from the 0^{th} range cell to 70^{th} range cell for different situations of the SCR. It can be seen that the JDL-MCFAR detectors using different measures can detect the target reliably. The KLD and LDD have the best detection performance and the HD has the worst detection performance.

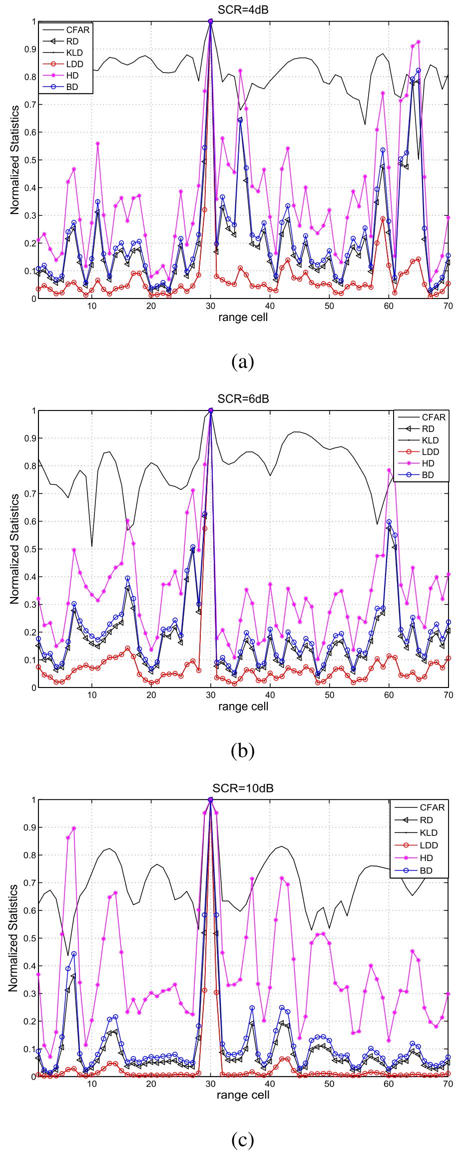

FIGURE 7. Normalized statistics in each range cell of different measures for different situations of SCR. (a) $SCR = 4dB$. (b) $SCR = 6dB$. (c) $SCR = 10dB$.

As the general analytical expressions of detection probability P_d and false-alarm probability P_{fa} are unavailable, the Monte Carlo method is used to obtain the threshold to maintain the false alarm rate constant. The test statistics without the target are calculated for 10^5 Monte Carlo simulations; thus, according to the P_{fa}, the detection threshold is determined. Figure 8 gives the probability of detection versus SCR for different P_{fa}. The P_{fa} values for the Figure 8 (a), (b), and (c) are 10^{-5}, 10^{-4}, and 10^{-3}, respectively.

The SCR is applied from -2dB to 16dB in intervals of 0.5dB. From the figures, it can be seen that the detectors

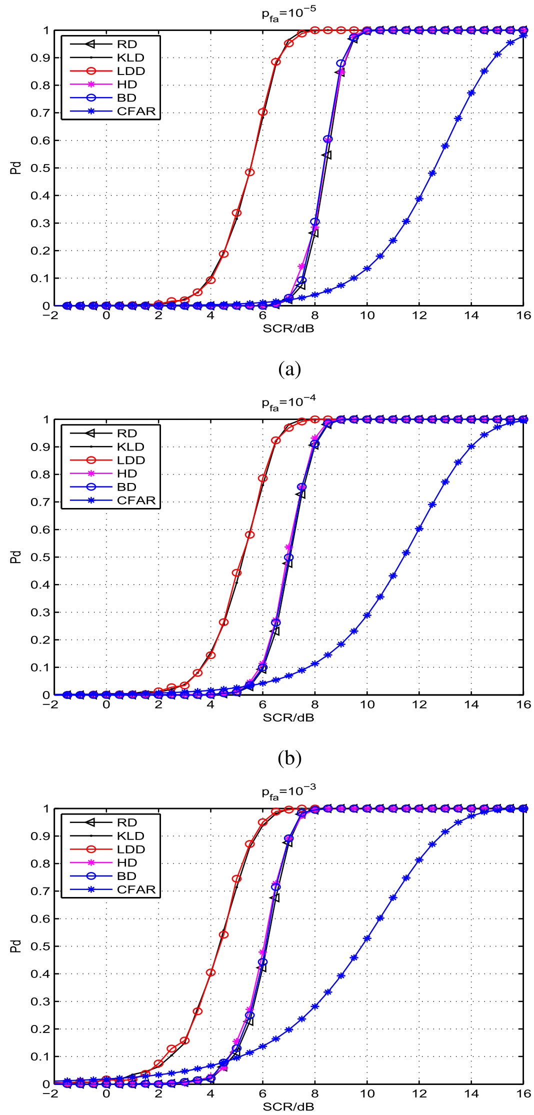

(a) (b) (c)

FIGURE 8. Detection probability versus SCR of different measures for different P_{fa}. (a) $P_{fa} = 10^{-5}$. (b) $P_{fa} = 10^{-4}$. (c) $P_{fa} = 10^{-3}$.

based on the JDL-MCFAR have better detection performance than the classical cell average CFAR (CA-CFAR) detector, and the KLD and LDD detectors have the best performance.

V. CONCLUSION

By obtaining multidimensional information from a signal through JDL processing, a novel detector named JDL-MCFAR detector is proposed here, which utilizes the geometry information of the signal. Five geometric measures have been used for the detectors, and the experiments show that the detectors based on these different measures can adequately detect the target for HFSWR. Moreover, the detectors based on KLD and LDD provide the best performance. Compared with the classical CA-CFAR detector, the JDL-MCFAR detector has better detection performance.

REFERENCES

[1] F. T. Berkey, ''Introduction to special section: Science and technology of over-the-horizon radar,'' *Radio Sci.*, vol. 33, no. 4, pp. 1043–1044, 1998.

[2] J. M. Headrick, ''Looking over the horizon (HF radar),'' *IEEE Spectr.*, vol. 27, no. 7, pp. 36–39, Jul. 1990.

[3] R. Srinivasan, ''Robust radar detection using ensemble CFAR processing,'' *IEE Proc.-Radar, Sonar Navigat.*, vol. 147, no. 6, pp. 291–297, Dec. 2000.

[4] M. D. E. Turley, ''Hybrid CFAR techniques for HF radar,'' in *Proc. Radar*, 1997, pp. 36–40.

[5] D. Ciuonzo, A. De Maio, and D. Orlando, ''A unifying framework for adaptive radar detection in homogeneous plus structured interference—Part I: On the maximal invariant statistic,'' *IEEE Trans. Signal Process.*, vol. 64, no. 11, pp. 2894–2906, Jun. 2016.

[6] D. Ciuonzo, A. De Maio, and D. Orlando, ''A unifying framework for adaptive radar detection in homogeneous plus structured interference—Part II: Detectors design,'' *IEEE Trans. Signal Process.*, vol. 64, no. 11, pp. 2907–2919, Jun. 2016.

[7] D. Ciuonzo, A. De Maio, and D. Orlando, ''On the statistical invariance for adaptive radar detection in partially homogeneous disturbance plus structured interference,'' *IEEE Trans. Signal Process.*, vol. 65, no. 5, pp. 1222–1234, Mar. 2017.

[8] H. Wang and L. Cai, ''On adaptive implementation of optimum MTI in severely nonhomogeneous environments,'' in *Proc. IEEE Int. Conf. Radar*, May 1990 pp. 351–355.

[9] H. Wang and L. Cai, ''A localized adaptive MTD processor,'' *IEEE Trans. Aerosp. Electron. Syst.*, vol. 27, no. 3, pp. 532–539, May 1991.

[10] H. Wang and L. Cai, ''On adaptive spatial-temporal processing for airborne surveillance radar systems,'' *IEEE Trans. Aerosp. Electron. Syst.*, vol. 30, no. 3, pp. 660–670, Jul. 1994.

[11] C. R. Rao, ''Information and the accuracy attainable in the estimation of statistical parameters,'' *Reson.-J. Sci. Edu.*, vol. 20, pp. 78–90, Jan. 2015.

[12] S. I. Amari, ''The EM algorithm and information geometry in neural network learning,'' *Neural Comput.*, vol. 7, no. 1, pp. 13–18, 1995.

[13] F. Gianfelici and V. Battistelli, ''Methods of information geometry (Amari, S. And Nagaoka, H.; 2000) [Book review],'' *IEEE Trans. Inf. Theory*, vol. 55, no. 6, pp. 2905–2906, Jun. 2009.

[14] J. Lapuyade-Lahorgue and F. Barbaresco, ''Radar detection using Siegel distance between autoregressive processes, application to HF and X-band radar,'' in *Proc. IEEE Radar Conf.*, May 2008, pp. 1–6.

[15] Y. Cheng, X. Wang, T. Caelli, X. Li, and B. Moran, ''On information resolution of radar systems,'' *IEEE Trans. Aerosp. Electron. Syst.*, vol. 48, no. 4, pp. 3084–3102, Oct. 2012.

[16] B. Ottersten, P. Stoica, and R. Roy, ''Covariance matching estimation techniques for array signal processing applications,'' *Digit. Signal Process.*, vol. 8, no. 3, pp. 185–210, Jul. 1998.

[17] H. Li, P. Stoica, and J. Li, ''Computationally efficient maximum-likelihood estimation of structured covariance matrices,'' in *Proc. IEEE Int. Conf. Acoust., Speech Signal Process.*, vol. 4, May 1998, pp. 2325–2328.

[18] P. Stoica, P. Babu, and J. Li, ''New method of sparse parameter estimation in separable models and its use for spectral analysis of irregularly sampled data,'' *IEEE Trans. Signal Process.*, vol. 59, no. 1, pp. 35–47, Jan. 2011.

[19] F. Hiai and D. Petz, ''Riemannian metrics on positive definite matrices related to means,'' *Linear Algebra Appl.*, vol. 436, nos. 11–12, pp. 2117–2136, 2008.

[20] R. Bhatia, *Positive Definite Matrices*. Princeton, NJ, USA: Princeton Univ. Press, 2015.

[21] H. Wolkowicz, R. Saigal, and L. Vandenberghe, *Handbook of Semidefinite Programming: Theory, Algorithms & Applications*. Norwell, MA, USA: Kluwer, 2000.

[22] T. M. Cover and J. A. Thomas, *Elements of Information Theory*. Beijing, China: Tsinghua Univ. Press, 2003.

[23] C. Stein, ''Inadmissibility of the usual estimator for the mean of a multivariate normal distribution,'' in *Proc. Berkeley Symp. Math. Statist. Probab.*, 1955, pp. 197–206.

[24] M. Charfi, Z. Chebbi, M. Moakher, and B. C. Vemuri, *Using the Bhattacharyya Mean for the Filtering and Clustering of Positive-Definite Matrices*. Berlin, Germany: Springer, 2013.

[25] H. M. Anver, ''Mean Hellinger distance as an error criterion in univariate and multivariate kernel density estimation,'' Ph.D. dissertations, Dept. Math., Southern Illinois Univ., Carbondale, IL, USA, 2010.

[26] S. I. Amari, ''Information geometry on hierarchy of probability distributions,'' *IEEE Trans. Inf. Theory*, vol. 47, no. 5, pp. 1701–1711, Jul. 2001.

[27] K. M. Carter, R. Raich, W. G. Finn, and I. A. O. Hero, "FINE: Fisher information nonparametric embedding," *IEEE Trans. Pattern Anal. Mach. Intell.*, vol. 31, no. 11, pp. 2093–2098, Nov. 2009.
[28] J. Weickert and H. Hagen, "Visualization and processing of tensor fields," in *Mathematics and Visualization*, vol. 8. Berlin, Germany: Springer-Verlag, 2005, pp. 129–145.
[29] F. Barbaresco, "Interactions between symmetric cone and information geometries: Bruhat-tits and Siegel spaces models for high resolution autoregressive Doppler imagery," in *Emerging Trends in Visual Computing*, vol. 5416, F. Nielsen, Ed. Berlin, Germany: Springer-Verlag, 2009, pp. 124–163.
[30] C. Stein, "Inadmissibility of the usual estimator for the mean of a multivariate normal distribution," in *Proc. Berkeley Symp. Math. Statist. Probab.*, 1955, pp. 197–206.
[31] X. Pennec, "Intrinsic statistics on Riemannian manifolds: Basic tools for geometric measurements," *J. Math. Imag. Vis.*, vol. 25, pp. 127–154, Jul. 2006.
[32] C. Lenglet, M. Rousson, R. Deriche, and O. Faugeras, "Statistics on the manifold of multivariate normal distributions: Theory and application to diffusion tensor MRI processing," *J. Math. Imag. Vis.*, vol. 25, no. 3, pp. 423–444, 2006.
[33] X. Hua, Y. Cheng, H. Wang, Y. Qin, and Y. Li, "Geometric means and medians with applications to target detection," *IET Signal Process.*, vol. 11, no. 6, pp. 711–720, 2017.
[34] X. Zhang, Q. Yang, and W. Deng, "Weak target detection within the nonhomogeneous ionospheric clutter background of HFSWR based on STAP," *Int. J. Antennas Propag.*, vol. 2013, Aug. 2013, Art. no. 382516.
[35] A. Aubry, A. D. Maio, L. Pallotta, and A. Farina, "Covariance matrix estimation via geometric barycenters and its application to radar training data selection," *IET Radar, Sonar Navigat.*, vol. 7, no. 6, pp. 600–614, Jul. 2013.

LEI YE received the B.S. degree in electronic information engineering and the M.S. degree in underwater acoustic engineering from Harbin Engineering University, Harbin, China, in 2011 and 2014, respectively. He is currently pursuing the Ph.D. degree in information and communication engineering with the Harbin Institute of Technology. His research interests include signal processing, target detection, and information geometry method.

QIANG YANG received the B.S., M.S., and Ph.D. degrees in information and communication engineering from the Harbin Institute of Technology, Harbin, China, in 1992, 1996, and 2002, respectively. He is currently the Professor with the School of Electronic Engineering, Harbin Institute of Technology. His research has been supported by the National Natural Science Council. He has authored or co-authored more than 30 papers in various journals and conferences. He is currently involved in weak target detection, real-time processing, and information extraction.

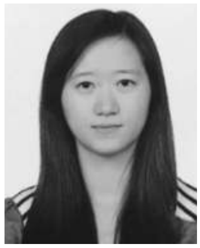

QIUSHI CHEN received the M.S. degree from the College of Underwater Acoustic Engineering, Harbin Engineering University, in 2013. She is currently pursuing the Ph.D. degree with the Department of Electronic and Information Engineering, Harbin Institute of Technology. Her research interest includes radar signal processing and compressive sensing.

WEIBO DENG received the B.S. degree in radio technology from Tsinghua University, Beijing, China, in 1984, and the M.S., and Ph.D. degrees in information and communication engineering from the Harbin Institute of Technology, Harbin, China, in 1992 and 2002, respectively. He is currently the Director and a Professor with the School of Electronic Engineering, Harbin Institute of Technology. He has authored or co-authored more than 60 papers published in international conferences and journals. His research interests include radar signal processing, clutter suppression, radar target scattering characteristics, antenna design, and compressed sensing. He is a Senior Member of the Chinese Institute of Electronics.